



RESEARCH ARTICLE

Regional hippocampal vulnerability in early multiple sclerosis: Dynamic pathological spreading from dentate gyrus to CA1

Vincent Planche^{1,2,3}  | Ismail Koubiyr^{1,2} | José E. Romero⁴ | José V. Manjon⁴ | Pierrick Coupé⁵  | Mathilde Deloire³ | Vincent Dousset^{1,2,3} | Bruno Brochet^{1,2,3} | Aurélie Ruet^{1,2,3} | Thomas Tourdias^{1,2,3}

¹Univ. Bordeaux, Bordeaux F-33000, France

²Inserm U1215 - Neurocentre Magendie, Bordeaux F-33000, France

³CHU de Bordeaux, Bordeaux F-33000, France

⁴Instituto Universitario de Tecnologías de la Información y Comunicaciones (ITACA), Universitat Politècnica de València, Camino de Vera s/n, Valencia 46022, España

⁵Laboratoire Bordelais de Recherche en Informatique, UMR CNRS 5800, PICTURA, Talence F-33405, France

Correspondence

Vincent Planche, Neurocentre Magendie, Inserm U1215, 146 Rue Léo Saïgnat, 33000 Bordeaux, France.
Email: planche.vincent@gmail.com

Funding information

ARSEP Foundation; Bordeaux University Hospital; TEVA Laboratories; French Agence Nationale de la Recherche, Grant/Award Numbers: ANR-10-LABX-57, ANR-10-LABX-43, ANR-10-IDEX-03-02, ANR-10-COHO-002; UPV, Grant/Award Numbers: UPV2016-0099, TIN2013-43457-R; Ministerio de Economía y competitividad

Abstract

Background: Whether hippocampal subfields are differentially vulnerable at the earliest stages of multiple sclerosis (MS) and how this impacts memory performance is a current topic of debate.

Method: We prospectively included 56 persons with clinically isolated syndrome (CIS) suggestive of MS in a 1-year longitudinal study, together with 55 matched healthy controls at baseline. Participants were tested for memory performance and scanned with 3 T MRI to assess the volume of 5 distinct hippocampal subfields using automatic segmentation techniques.

Results: At baseline, CA4/dentate gyrus was the only hippocampal subfield with a volume significantly smaller than controls ($p < .01$). After one year, CA4/dentate gyrus atrophy worsened (-6.4% , $p < .0001$) and significant CA1 atrophy appeared (both in the stratum-pyramidale and the stratum radiatum-lacunosum-moleculare, -5.6% , $p < .001$ and -6.2% , $p < .01$, respectively). CA4/dentate gyrus volume at baseline predicted CA1 volume one year after CIS ($R^2 = 0.44$ to 0.47 , $p < .001$, with age, T2 lesion-load, and global brain atrophy as covariates). The volume of CA4/dentate gyrus at baseline was associated with MS diagnosis during follow-up, independently of T2-lesion load and demographic variables ($p < .05$). Whereas CA4/dentate gyrus volume was not correlated with memory scores at baseline, CA1 atrophy was an independent correlate of episodic verbal memory performance one year after CIS ($\beta = 0.87$, $p < .05$).

Conclusion: The hippocampal degenerative process spread from dentate gyrus to CA1 at the earliest stage of MS. This dynamic vulnerability is associated with MS diagnosis after CIS and will ultimately impact hippocampal-dependent memory performance.

KEYWORDS

clinically isolated syndrome, cognition, dentate gyrus, hippocampus, hippocampal subfields, MRI, multiple sclerosis

1 | INTRODUCTION

Patients with multiple sclerosis (MS) are often afflicted with episodic memory impairment and, over the past decade, a growing number of studies have investigated how hippocampal abnormalities might be related to this deficit (Dutta et al., 2011; Hulst et al., 2015; Planche et al., 2017a; Sicotte et al., 2008). Postmortem anatomopathological

analyses of MS brains, together with studies on animal models of MS, have described early microglial activation, neuronal loss, synaptic dysfunction and demyelination within different regions of the hippocampus (Dutta et al., 2011; Papadopoulos et al., 2009; Planche et al., 2017b). However, the time course of these alterations and the interrelations between the different types of cellular modifications during the evolution of the disease remain largely unknown.

One way to isolate pathogenic mechanisms within the hippocampal circuit is to study its regional vulnerability (Small, 2014). Indeed, the

Aurélie Ruet and Thomas Tourdias contributed equally to this work

hippocampus is composed of distinct subfields whose morphological, cellular, molecular, functional, and connectivity profiles are very different: the dentate gyrus, the cornu ammonis (CA, with subdivisions from CA1 to CA4) and the subiculum. Initially used to study Alzheimer's disease and physiological aging (West, Coleman, Flood, & Troncoso, 1994), this approach of interrogating differentially the malfunctioning hippocampal circuit has been adapted more recently to investigate MS (Gold et al., 2010; Longoni et al., 2015; Rocca et al., 2015; Sicotte et al., 2008).

Regarding MRI studies, the differential vulnerability of one hippocampal subfield compared to the others during the course of MS remains controversial. Indeed, some authors have highlighted the differential vulnerability of CA1 (Longoni et al., 2015; Sicotte et al., 2008) and others the vulnerability of CA3/CA4/dentate gyrus (Gold et al., 2010; Rocca et al., 2015). The reasons for discrepancies between studies remain speculative but they might be explained by the heterogeneity of the measurement methods used (surface-based mesh modelling and volumetric analyses) and/or by the heterogeneity of the populations studied (relapsing MS with different disease durations and/or progressive MS). This latter point seems crucial if we postulate that the pattern of atrophy of hippocampal subfields changes according to disease progression. Previous studies have so far been unable to test such timing and the dynamics of differential hippocampal subfield damage because of cross-sectional design. It is also important to note that none of these works investigated clinically isolated syndrome (CIS), which is required to address the question of the differential vulnerability of hippocampal subfields to the earliest pathophysiological mechanisms in MS. Indeed, CIS is the first demyelinating event suggestive of a future relapsing-remitting MS, that will be formally defined later on by the dissemination in time and space of demyelinating lesions (Polman et al., 2011; Miller, Chard, & Ciccarelli, 2012). Thus, studying persons with CIS offers a unique opportunity to understand the "first steps" of the pathophysiological mechanisms leading to MS.

By analogy with other neurodegenerative diseases (de Flores, La Joie, & Chételat, 2015; Maruszak and Thuret, 2014), we hypothesize here that hippocampal degeneration in persons with CIS and early MS is not uniform and that pathological alterations will spread from one hippocampal subfield to the others in a process leading to diffuse hippocampal atrophy. To test this hypothesis, we measured the volumes of five distinct hippocampal subfields longitudinally, using advanced 3 T MRI-based automatic segmentation techniques, and analyzed the dynamics of atrophy of these subfields together with their clinical and neuropsychological correlates.

2 | METHODS

2.1 | Participants

Fifty-six persons with CIS (PwCIS) were prospectively enrolled between 2 and 6 months after an initial clinical event compatible with a demyelinating inflammatory syndrome: a monofocal and monophasic neurological symptom that can be related to an optic nerve, spinal cord, brainstem, cerebral hemisphere, or cerebellum lesion (Miller et al.,

2012). Patients were assessed by neuropsychological testing and MRI at baseline and at 1-year follow-up. At baseline, at least two clinically silent lesions with a minimum diameter of 3 mm were required for inclusion. One of these lesions had to be cerebral (ovoid or periventricular), while the other could be located in the spine or brain. None of the patients were treated with disease-modifying therapy at inclusion. Contraindications to MRI, the presence of other neurological, psychiatric or systemic diseases, steroid treatment within one month, starting or stopping antidepressants or anxiolytic treatments within 2 months of MRI, and neuropsychological examination were considered as exclusion criteria. During the follow-up period of one year, the diagnosis of multiple sclerosis was confirmed (or not) by the treating physician according to the 2010 McDonald criteria (Polman et al., 2011).

Fifty-five healthy controls (HC), free of neurological, psychiatric, or systemic diseases, and drug or alcohol abuse, were also included. They were tightly matched for age, gender, and educational level to PwCIS, to calculate cognitive z-scores both at baseline and one year after (see below). Among these 55 controls, a subgroup of 38 HC (still matched with the CIS group, see Table 1) underwent MRI at baseline but they were not rescanned at year 1.

All subjects were prospectively enrolled from 2012 to 2015 at our MS center. Written informed consent was obtained prior to participation. This study was approved by the local institutional ethics review board and registered in Clinicaltrials.gov (NCT01865357).

2.2 | Neuropsychological testing

To assess hippocampal functions, PwCIS and HC performed the Selective Reminding Test (SRT) for episodic verbal memory performance and the Brief Visuospatial Memory Test (BVMT-R) to test episodic visuospatial memory performance. Each PwCIS was compared with the HC group at the appropriate time point to calculate a z-score for each test at each time point. To take into account practice effects, the scores of PwCIS at baseline were compared with the mean score of the HC group obtained at baseline, while the scores of PwCIS at 1 year were compared with the mean score of the HC group obtained during their second session of neuropsychological testing at 1 year. The z-scores of each SRT and BVMT-R subtest were averaged to calculate one composite verbal memory score and one composite visuospatial memory score. Lower z-scores indicate lower performance. A patient was considered impaired in a given cognitive domain if his/her score was below the fifth percentile (i.e., z-score < -1.64).

2.3 | MRI acquisition and analyses

Participants were scanned on a 3 T MRI system at our MS centre (either Philips Achieva or GE Medical Systems Discovery MR 750w). Thirteen patients (out of 46, i.e., 28%) were not scanned on the same machine at baseline and after one year (Philips Achieva at baseline and GE Discovery after 1 year). The imaging protocol was harmonized between magnets and included the same 3D gradient-echo T1-weighted sequence (TR/TE/TI/flip angle = 8.2 ms/3.5 ms/982 ms/7°, resolution 1 × 1 × 1 mm, 256 mm FOV) and a 2-D axial Fluid

TABLE 1 Clinical, neuropsychological, and general MRI features of the studied populations

	Controls with MRI (n = 38)	CIS baseline (n = 56)	CIS 1-year (n = 46)	p value
Demographic and clinical features				
Mean age, years [SD]	36.6 [10.7]	36.5 [11.2]	-	0.94
Sex ratio (F/M)	26/12	46/10	-	0.14
Education level (high/low ^a)	27/11	39/17	-	0.88
Median EDSS score [range]	-	1.0 [1.0–6.0]	1.0 [1.0–6.0]	0.63
Conversion to MS	-	-	30/46 (65.2%)	-
Neuropsychological features				
Median verbal memory z-score [range] [% impaired]		0.10 [−4.9 to 1.0] {7.4%}	−0.13 [−3.7 to 1.2] {10.7%}	0.91
Median visuospatial memory z-score [range] [% impaired]		−0.20 [−5.2 to 0.82] {17.9%}	0.10 [−3.5 to 1.0] {6.5%}	0.02
Imaging features				
Median T2 lesion volume, mL [range]	-	0.73 [0.02–63.12]	1.08 [0.06–67.74]	0.67
Mean normalized brain volume, % [SD]	86.4 [3.2]	85.1 [3.9]	83.9 [4.1]	0.21 ^b /0.012 ^c

Note. Abbreviations: CIS = Clinically Isolated Syndrome; EDSS = Expanded Disability Status Scale; MS = multiple sclerosis; SD = standard deviation.

^aEducation level was considered as high or low according to French baccalaureate (equivalent to A-level).

^bControls vs CIS baseline.

^cCIS baseline vs CIS 1-year

Attenuated Inversion Recovery (FLAIR) sequence (TR/TE/TI = 11000 ms/140 ms/2800 ms, resolution $1 \times 1.1 \times 3$ mm, 230 mm FOV). Preliminary analyses (not shown) using the type of scanner as a covariate did not show any effect of the magnet on volumetric analyses.

Lesion load was determined by the lesion growth algorithm as implemented in the Lesion Segmentation Tool (LST) version 2.0.15 (<http://www.applied-statistics.de/lst.html>) in Statistical Parametric Mapping (SPM12) (Schmidt et al., 2012). To do this, T1 images were co-registered with FLAIR images to calculate lesion belief maps, thresholded with the same parameters for each patient ($\kappa = 0.3$). Binary maps of lesions were reviewed and corrected manually by two blinded experts (MR engineer and neurologist), using 3D Slicer 4.4.0 (www.slicer.org).

For the volumetric analyses of brain structures and hippocampal subfields, T1-weighted images were processed using the volBrain system (<http://volbrain.upv.es>) (Manjón and Coupé, 2016). After denoising with an adaptive nonlocal mean filter (Manjón, Coupé, Martí-Bonmatí, Collins, & Robles, 2010), images were affine-registered in the Montreal Neurological Institute (MNI) space using ANTS software (Avants et al., 2011), corrected for image inhomogeneities using N4 (Tustison et al., 2010) and finally intensity-normalized (Nyúl and Udupa, 1999). Then, the hippocampal subfields were segmented based on a multiatlas framework combining nonlinear registration and patch-based label fusion (Romero, Coupe, & Manjón, 2016, 2017). This method uses a training library composed of 5 high-resolution T1-weighted images labelled manually according to the protocol proposed by Winterburn et al. (2013) which is one of the rare freely available atlases that specifically separate CA4/DG from CA2/3 on the one hand and CA1 neuritic and pyramidal layers on the other hand (Yushkevich et al., 2015). The 3D-T1-weighted images of the subjects considered in this study ($1 \times 1 \times 1$ mm³) were up-sampled to the image resolution of the training library ($0.5 \times 0.5 \times 0.5$ mm³) using the local adaptive super-resolution (LASR) method (Coupé, Manjón, Chamberland, Descoteaux,

& Hiba, 2013). The method finally provided automatic segmentation of hippocampal subfields gathered into 5 labels: subiculum, CA1-SP (stratum pyramidale), CA1-SRLM (stratum radiatum-lacunosum-moleculare), CA2/3 and CA4/dentate gyrus (Figure 1), allowing us to test our *a priori* hypotheses regarding the selective vulnerability of the dentate gyrus or CA1, as suggested in the literature from animal, neuropsychological (using pattern separation tasks) and MRI studies (Planche et al., 2017b, c; Rocca et al., 2015; Sicotte et al., 2008). In our previous paper, the hippocampal subfield segmentation accuracy using T1-weighted has been estimated to be 62% for the Winterburn protocol in terms of average DICE coefficient. Moreover, the whole hippocampus segmentation accuracy has been estimated to 88% in term of DICE coefficient. Finally, it has been shown that super-resolution enables to obtain an accuracy close the one obtained when using high resolution T1 (Romero et al., 2017). Every up-sampled image and every subfield label were quality-controlled and manually corrected by a blinded neurologist if needed (in the case of inappropriate inclusion of parahippocampal T1-hypointense lesions (Supporting Information, Figure 1), choroidal plexus and/or CSF “pockets,” using 3D Slicer 4.4.0 (www.slicer.org)). To control for variations in head size, the volumes of hippocampal subfields were normalized using the intracranial cavity volume of each subject (Manjón et al., 2014). Normalized brain volume (NBV) was also calculated as the sum of cerebral white and grey matters, divided by the intracranial cavity volume of each subject.

2.4 | Statistical analyses

Statistical analyses were performed with Prism software 6 (Graphpad) and XLstats 19.4 (Addinsoft). The distribution of all continuous data was tested with the Shapiro–Wilk normality test. We first compared clinical, neuropsychological, and imaging characteristics between HC and PwCIS at baseline by using Fisher’s exact tests for categorical

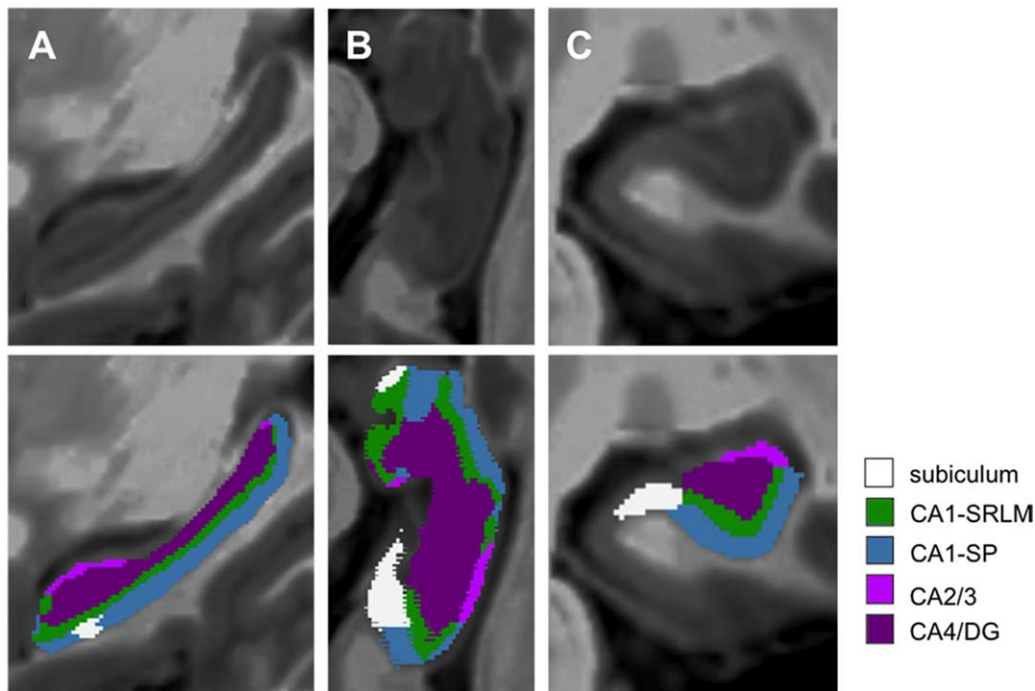


FIGURE 1 Segmentation of the five hippocampal subfields. Super-resolution T1-weighted images ($0.5 \times 0.5 \times 0.5 \text{ mm}^3$) centered on the left hippocampus of a patient with clinically isolated syndrome (PwCIS) in the sagittal plane (a), in an oblique axial cut parallel to the plane of the hippocampus (b) and in the coronal plane (c). Five hippocampal subfields were automatically segmented (and manually corrected if needed) according to the atlas of Winterburn et al.: the subiculum, the stratum pyramidale of CA1 (CA1-SP), the stratum-lacunosum-moleculare of CA1 (CA1-SRLM), CA2/3, and CA4/dentate gyrus (CA4/DG) [Color figure can be viewed at wileyonlinelibrary.com]

variables, and unpaired *t* tests or Mann–Whitney tests for ordinal variables. The comparisons of baseline and 1-year characteristics of PwCIS were done with paired *t* tests or Wilcoxon tests, as appropriate.

To compare the volumes of the 5 hippocampal subfields between groups, we first performed an analysis of variance, followed by a Sidak multiple comparisons test. Cohen’s *d* was used to measure the effect size of atrophy between patients and HC, whereas annualized rate of atrophy was used to compare PwCIS at year 1 and baseline.

Then, because the decreases in subfield volumes were consistent between right and left hippocampi, further statistical analyses were performed on the sum of right and left subfield volumes to avoid multiple comparisons. Relationships between neuropsychological scores, demographic, clinical, and imaging variables were assessed using correlation coefficients (Pearson or Spearman according to statistical distribution). The associations were further tested in multivariate context. To this end, (i) hippocampal subfields volumes at year 1, (ii) MS diagnosis after 1-year follow-up, and (iii) memory performance (dependent variables) were predicted with hierarchical regression models, including two hierarchical blocks. In the first block, relevant demographical, clinical, and general MRI features known as nuisance variables were systematically forced into the model. In the second block, the volumes of hippocampal subfields were added to the variables of the first block. The predictive power of the two blocks was compared by using the Akaike information criterion (AIC). A linear regression model was used whenever possible while logistic regression was seen as the appropriate alternative for categorical/binomial outcome variables. All tests were two-tailed, with a global type I error set at $\alpha = 0.05$.

3 | RESULTS

3.1 | Demographic, clinical, and general MRI features of participants

A total of 56 PwCIS and 55 HC were included. At baseline, all PwCIS and HC were tested with the neuropsychological battery while all PwCIS but only a subgroup 38 HCs were assessed with MRI. At year 1, because 10 patients were lost to follow-up, 46 PwCIS were retested with the same neuropsychological battery and rescanned with the same imaging protocol. All the 55 HCs were retested with the same neuropsychological battery but they were not rescanned at year 1.

The CIS and HC groups were comparable for age, sex, and educational level (Table 1). In this cohort of patients, after one year, 65.2% of PwCIS were diagnosed with MS according to the 2010 McDonald criteria.

In PwCIS, there was no significant difference between baseline and 1 year follow-up regarding disability (Expanded Disability Status Scale, EDSS) and T2-lesion load. Neuropsychological testing was also rather stable between baseline and 1 year follow-up, except for the episodic visuospatial memory score that had even slightly increased ($p = .02$) (Table 1). Normalized brain volume (NBV) significantly decreased during this period (-1.4% , $p = .012$).

3.2 | Dynamics of regional hippocampal vulnerability

At baseline, hippocampal volumes were significantly lower in PwCIS compared to controls only in the CA4/dentate gyrus subfield (Figure

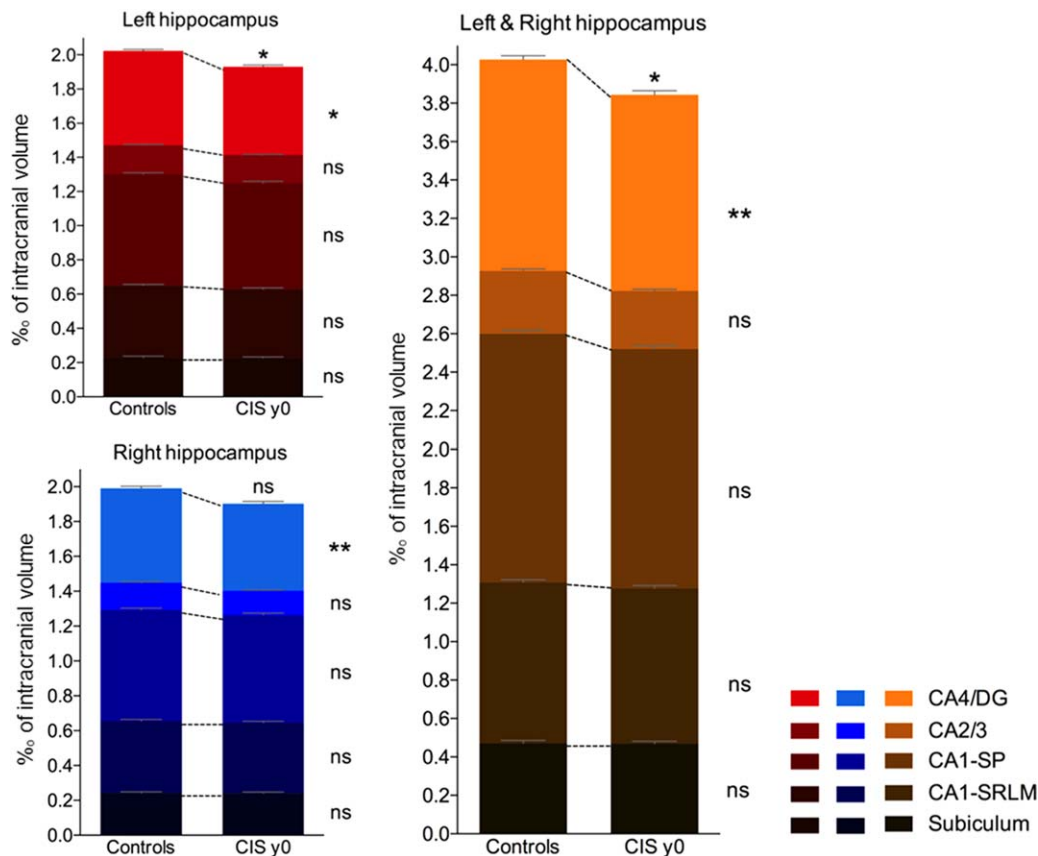


FIGURE 2 Comparison of the normalized volumes of hippocampal subfields between healthy controls and persons with clinically isolated syndrome (CIS) at baseline (y0). Histograms represent the cumulative volumes of all the left hippocampal subfields (in red), of all the right hippocampal subfields (in blue) and of all right and left hippocampal subfields (in orange). The color gradient represents individual hippocampal subfields. ns = nonsignificant, * $p < .05$, ** $p < .01$ (corrected for multiple comparisons) [Color figure can be viewed at wileyonlinelibrary.com]

2). This was consistently true for the left ($-6.5%$, $d = 0.53$, $p < .05$) and for the right hippocampus ($-7.7%$, $d = 0.54$, $p < .01$) and when both sides were pooled together ($-7.2%$, $d = 0.58$, $p < .01$). In PwCIS, this atrophy of CA4/dentate gyrus was not correlated with age, disability, or T2 lesion load at baseline.

Follow-up data after one year compared to baseline measures showed that the normalized volumes of CA4/dentate gyrus ($-6.4%$, $p < .001$), CA1-SP ($-5.6%$, $p < .01$), and CA1-SRLM ($-6.2%$, $p < .05$) significantly decreased in both sides. No significant atrophy was found in the subiculum or CA2/3 subfields (Figure 3).

As the atrophy of CA1 subfield chronologically succeeded the atrophy of CA4/dentate gyrus, this suggests that the same pathophysiological process spreads from CA4/dentate gyrus to CA1 in individual patients. To test this hypothesis, we designed a hierarchical linear regression model to test how CA1-SP, CA1-SRLM and whole hippocampus volumes at year 1 (dependent variables) can be predicted by the volume of CA4/dentate gyrus at baseline (while first taking into account confounders such as age, T2 lesion-load and NBV in the model). We found that CA4/dentate gyrus at baseline improved the statistical prediction of CA1 volumes at year 1 from $R^2 = 0.19$ (when considering usual factors such as age, T2 lesions and NBV) to $R^2 = 0.44$ ($AIC_{block2} < AIC_{block1}$). It also predicted the whole hippocampal volume

one year afterwards independently of age, T2 lesions or NBV (Table 2). CA4/DG remained a significant and independent correlate of CA1 and whole hippocampal volumes at year 1, although other hippocampal subfields (subiculum and CA2/3) were introduced in the model ($\beta = 0.34$, $p = .018$ for CA1-SP and $\beta = 0.39$, $p < .001$ for the whole hippocampus, respectively). Altogether, a smaller focal volume at baseline predicted smaller global volumes at year 1, which points to a pathological continuum starting within CA4/dentate gyrus and spreading progressively and more globally to CA1.

3.3 | Relationship between the atrophy of hippocampal subfields and clinical outcomes

To study the link between the early vulnerability of CA4/dentate gyrus and the pathophysiological process specific to MS, we first investigated whether CA4/dentate gyrus volume at baseline would be able to predict MS diagnosis at year 1. Using univariate analyses, we found that both T2-lesion load and CA4/dentate gyrus volume were significantly associated MS diagnosis after 1-year follow-up ($p = .002$ and $p = .014$, respectively). A multiple logistic regression model showed that the volume of CA4/dentate gyrus at baseline was the only factor independently associated with future MS diagnosis ($\beta = 0.57$, $p = .025$ and

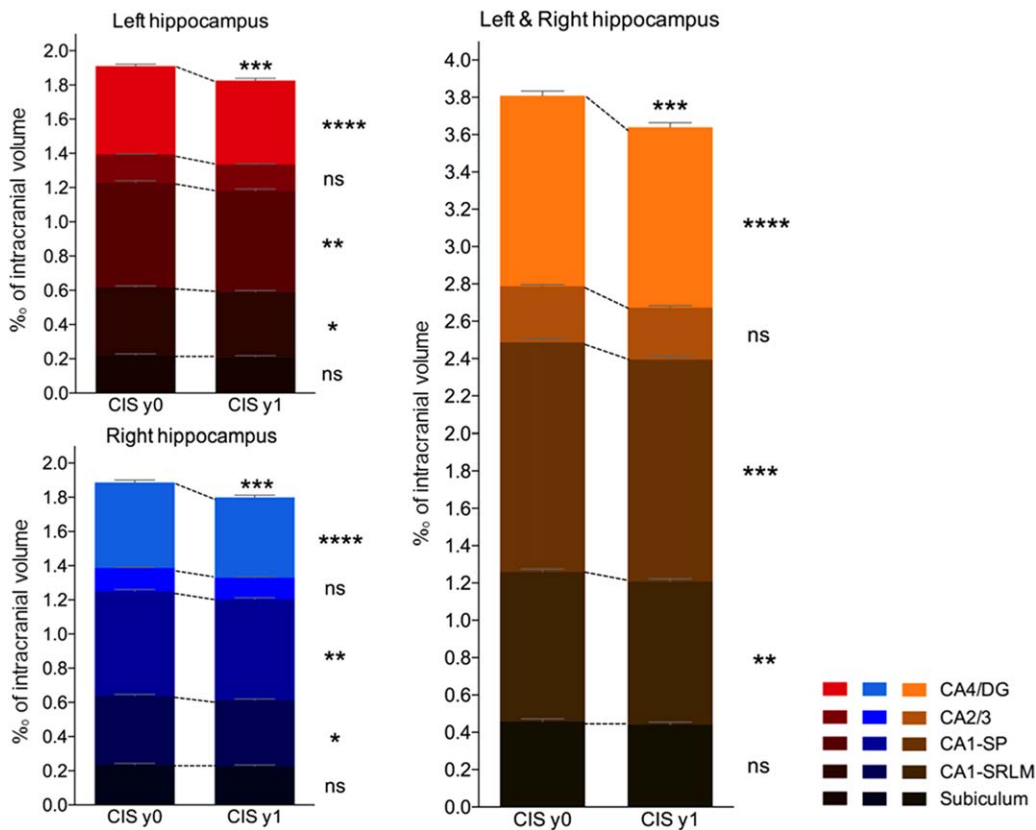


FIGURE 3 Comparison of the normalized volumes of hippocampal subfields between persons with clinically isolated syndrome (CIS) at baseline (y0) and 1-year follow-up (y1). The histograms represent the cumulative volumes of all the left hippocampal subfields (in red), of all the right hippocampal subfields (in blue) and of all right and left hippocampal subfields (in orange). The color gradient represents individual hippocampal subfields. ns = nonsignificant, * $p < .05$, ** $p < .01$, *** $p < .001$, **** $p < .0001$ (corrected for multiple comparisons) [Color figure can be viewed at wileyonlinelibrary.com]

$R^2 = 0.28$, $p = .016$) while age, gender, EDSS, T2-lesion load, and NBV were not predictive.

Finally, we investigated whether early hippocampal regional vulnerability had a clinical impact on episodic memory performance. The results of univariate correlations and regression models between memory scores and demographic, clinical, and imaging data at baseline and year 1 are presented in Table 3. According to multivariate analyses, no model was able to explain memory performance at baseline. The volume of CA1-SP and the educational level of patients were independent predictors of the episodic verbal memory composite score at year 1 ($\beta = 0.87$, $p = .042$ and $\beta = 0.51$, $p = .031$, respectively).

4 | DISCUSSION

We demonstrated in this study that the CA4/dentate gyrus subfield of the hippocampus is the first subfield to be atrophied across the course of MS, at the stage of CIS. This pattern of regional hippocampal atrophy worsens during the first year of disease evolution and spreads within CA1 (both in the cell bodies layer CA1-SP and the neuritic layers CA1-SRLM). CA4/dentate gyrus volume at baseline was associated with diagnosis of MS one year afterward. Whereas isolated CA4/dentate gyrus atrophy at the stage of CIS failed to correlate with memory scores, it predicted the extension of the pathological process within

CA1 one year later, which was in turn correlated with episodic verbal memory performance, independently of usual confounders.

Our main finding of a “natural history” of hippocampal subfield degeneration in MS, from dentate gyrus to CA1, is supported by anatomical and functional studies in both human and animal models of the disease. First, we previously reported that pattern separation performance—a cognitive task critically dependant on dentate gyrus function (Bakker, Kirwan, Miller, & Stark, 2008)—was decreased in patients with CIS and early MS, when conventional visuospatial episodic memory tests (BVM-T-R) were not yet altered, suggesting an early and isolated dentate gyrus dysfunction during the course of the disease (Planche et al., 2017c). Such functional alterations suggested by the pattern separation task are therefore consolidated by the anatomical alterations observed in this MRI study. Second, our findings are also supported by a previous work showing that dentate gyrus structure and function are selectively disrupted by microglial activation at the early stage of experimental autoimmune encephalomyelitis (EAE, the animal model of MS) (Planche et al., 2017b). The independent association we found here between CA4/dentate gyrus volume at the stage of CIS and the diagnosis of MS one year after CIS also suggests this link between dentate gyrus damage and the early diffuse pathophysiological process specific to MS. Third, the vulnerability of the dentate gyrus, prior to other hippocampal subfields at the early stage of MS, could be explained by its

TABLE 2 Univariate correlations and hierarchical linear regression models between volumes of CA1 subfields or whole hippocampal volume at year 1 (dependent variables) and volume of CA4/dentate gyrus at baseline

1 year volume		Explanatory variables (at baseline)	Univariate analysis (<i>r</i>)	Multivariate analysis (β)	Adjusted multivariate model (R^2)
CA1-SP	Block 1	Age	−0.16	ns	0.19 [†]
		T2LL	−0.21	ns	
		NBV	0.44**	0.47 [†]	
	Block 2	Age	−0.16	ns	0.44**** ^a
		T2LL	−0.21	ns	
		NBV CA4/DG	0.44** 0.63***	ns 0.40***	
CA1-SRLM	Block 1	Age	−0.06	ns	0.27**
		T2LL	−0.16	ns	
		NBV	0.48***	0.64***	
	Block 2	Age	−0.06	ns	0.47**** ^a
		T2LL	−0.16	ns	
		NBV CA4/DG	0.48*** 0.62***	0.40 [†] 0.47***	
Hippocampus	Block 1	Age	−0.16	ns	0.32**
		T2LL	−0.26	ns	
		NBV	0.56***	0.65***	
	Block 2	Age	−0.16	ns	0.61**** ^a
		T2LL	−0.26	ns	
		NBV CA4/DG	0.56*** 0.71***	0.37 [†] 0.58***	

Note. Abbreviations: CA1-SP = CA1-stratum pyramidale; CA1-SRLM = CA1-stratum radiatum-lacunosum-moleculare; CA4/DG = CA4/dentate gyrus; NBV = normalized brain volume; T2LL = T2 lesion load; ns = nonsignificant.

Age, T2LL, and NBV were entered into an initial model (block 1) as nuisance variables.

^aAIC_{block2} < AIC_{block1}

* $p < .05$, ** $p < .01$, *** $p < .001$.

particular anatomical location. Indeed, it is adjacent to cerebrospinal fluid (CSF) spaces (third ventricle in rodents and choroidal fissure in humans) where cytokines and immune cells preferentially penetrate the hippocampus, as suggested experimentally in EAE (Habbas et al., 2015). We postulate that the hierarchical vulnerability of hippocampal subfields in MS might be better explained by their anatomical contiguity rather than by a network-dependent disposition, as in Alzheimer's disease for instance (Kerchner et al., 2013). A gradient of infiltrating immune cells and cytokines would diffuse progressively from the CSF to the dentate gyrus, then to CA1, and probably to the whole medial temporal lobe. In this model, the progression of the disease from the dentate gyrus to CA1 might be slowed down by the presence of the vestigial intrahippocampal sulcus, potentially explaining the delay between dentate gyrus and CA1 atrophy reported in this study. Additional experiments will be needed to test these mechanistic hypotheses.

From the anatomopathological point of view, our study also highlights the striking vulnerability of the hippocampus to neurodegeneration in the context of neuroinflammation. Indeed, the annualized rate of atrophy during the first year of the disease's evolution ranged from −5.6% to −6.4%, respectively for CA1 and CA4/dentate gyrus, whereas it was "only" −1.4% for the normalized brain volume in our population of PwCIS (which was in the upper range of what was usually observed in the literature on CIS and relapsing MS, that is, from −0.5% to −1.35% (Pérez-Miralles et al., 2013; De Stefano et al., 2014)). This selective and disproportionate hippocampal volume loss, in

excess to global brain atrophy, has already been observed in a seminal cross-sectional study on patients with relapsing and progressive MS (Sicotte et al., 2008). The annualized rate of hippocampal atrophy we report here (−5.9%) is even in the upper range of what has been reported for patients with Alzheimer's disease or mild cognitive impairment (−3.5% to −6%/year) (Du et al., 2004; Jack et al., 2000; Wang et al., 2003) and far beyond what has been reported for physiological aging (−0.8% to −2.3%/year) (Jack et al., 2011).

Besides these anatomical considerations, we also questioned the link between the early regional vulnerability of the hippocampus and memory impairment in MS. On the one hand, the CA4/dentate gyrus atrophy observed at baseline was not correlated with episodic memory performance in our cohort. Although we have to take into account that the memory abilities of the PwCIS included in this study were not severely affected (regarding the median z-scores and the percentage of impaired patients), we postulate that CA4/dentate gyrus atrophy at the stage of CIS is "not enough" to explain the memory decline observed in "global" episodic memory tests such as the SRT or the BVMT-R. Perhaps more specific tests such as the behavioral pattern separation task (Stark, Yassa, Lacy, & Stark, 2013) would have allowed us to pinpoint such a subtle memory decline related to CA4/dentate gyrus damage (Planche et al., 2017c) and future studies should address this point. On the other hand, we found that CA1 atrophy explained part of the "global" episodic verbal memory decline one year after inclusion, when diagnosis of MS was finally observed in 65.2% of the patients. This suggests that CA1 atrophy is the best anatomical correlate of memory

TABLE 3 Univariate correlations and hierarchical regression models between memory composite scores at baseline or after 1 year follow-up (dependent variables) and demographical, clinical, and MRI features

		Explanatory variables	Univariate analysis (<i>r</i>)	Multivariate analysis (β)	Adjusted multivariate model (R^2)	
Baseline						
Episodic verbal memory	Block 1	Age	-0.04	ns	ns	
		T2LL	-0.20	ns		
		NBV	0.12	ns		
		Education level	0.32*	0.38*		
	Block 2 ^a	-	-	-	-	
Episodic spatial memory	Block 1	Age	-0.18	ns	ns	
		T2LL	-0.18	ns		
		NBV	0.17	ns		
		Education level	0.32*	ns		
	Block 2 ^a	-	-	-	-	
1 year						
Episodic verbal memory	Block 1	Age	-0.15	ns	ns	
		T2LL	-0.14	ns		
		NBV	0.17	ns		
		Education level	0.24	ns		
	Block 2	Age	-0.15	ns		0.26*
		T2LL	-0.14	ns		
		NBV	0.17	ns		
		Education level	0.24	0.51*		
		CA1-SP	0.30*	0.87*		
		CA1-SRLM	0.24	ns		
Episodic spatial memory	Block 1	Age	-0.35*	ns	ns	
		T2LL	-0.17	ns		
		NBV	-0.03	ns		
		Education level	0.14	ns		
	Block 2 ^a	-	-	-	-	

Note. Abbreviations: CA1-SP = CA1-stratum pyramidale; CA1-SRLM = CA1-stratum radiatum-lacunosum-moleculare; T2LL = T2 lesion load; NBV = normalized brain volume; ns = nonsignificant.

Age, T2LL, NBV, and educational level were entered into an initial model (Block 1) as nuisance variables. Covariables related to hippocampal subfields were added in a second model (Block 2) according to univariate correlations (p value < .2) to predict memory scores.

^aBlock 2 was equivalent to Block 1 because no correlation (p < .2) was found between the volume of any hippocampal subfields and the memory score $*p$ < .05.

performance in MS, as previously described in cross-sectional studies including patients with relapsing and progressive MS (Longoni et al., 2015; Sicotte et al., 2008).

A recent cross-sectional study found an “expansion” of the dentate gyrus during MS (Rocca et al., 2015). The divergences between our findings and this previous work may be attributed to various points. Indeed, contrary to our work, this study investigated patients at a later stage of the disease, with relapsing and progressive MS, and it used a surface-based mesh modelling technique to study the shape of the hippocampus (Thompson et al., 2004). Using this technique, the authors found an outward displacement of the supero-medial hippocampal surface and concluded on a larger radial distance of the dentate gyrus in patients with MS. However, it should be borne in mind that when using such a method, measuring external surface modifications does not enable the direct characterization of the inner alterations of a particular subfield. It is not clear how the atrophy of the deepest regions of the hippocampus (such as the dentate gyrus, which is curled inside the Cornu Ammonis) would impact the outer surface of the structure. For instance, the expansion of CSF pockets due to atrophy within the hippocampal fissure/sulcus might result in tissue “expansion” on the supero-medial side of the hippocampus despite there being no real dentate gyrus “hypertrophy”. We also hypothesized that a shift of

rotation of the hippocampus due to atrophy would induce an outward displacement of part of the surface, introducing contradictory results. Thus, radial mapping provides valuable information on hippocampal surface change (i.e., CA1 and the subiculum) but should be interpreted with caution for inner structures such as the dentate gyrus (La Joie et al., 2010). The limits of these surface-based modelling strategies to assess hippocampal subfield anatomy have been discussed extensively in the field of Alzheimer’s disease and aging (de Flores et al., 2015; Morra et al., 2009), even by the authors who pioneered the method (Frisoni et al., 2008; Thompson et al., 2004). Therefore, proper volumetric analyses with manual or automatic segmentation are now considered more relevant than radial mapping to investigate hippocampal regional vulnerability, although they have their own limitations and require protocol harmonization to clearly define subfield boundaries (Wisse et al., 2017). For instance, we acknowledge that the Winterburn protocol we used here mainly delineates CA2/3 in its dorsal portion to increase segmentation reliability, although it can lead to volume underestimations. Therefore, our results might have differed by using other definitions of the hippocampal subfields boundaries. From the technical point of view, we also acknowledge that we only used T1-weighted images to label hippocampal subfields, whereas both T1 and T2-weighted images are often preferred to delineate internal boundaries,

especially for very thin layers such as CA1-SRLM. However pooling CA1-SRLM with the bigger CA1-SP would not have changed our main conclusions. Furthermore, we have recently validated that the single use of T1-weighted images up-sampled with local adaptive super-resolution leads to reliable hippocampal subfield labeling, compared to the combination of T1 and T2-weighted images (Romero et al., 2017).

The main limitation of our study is the lack of MRI follow-up for our healthy control group to clearly disentangle the contribution of time-dependent versus disease-dependent processes in our longitudinal measures of atrophy in the CIS group. However, our results on the dynamics of progressive hippocampal subfield atrophy are likely related to the disease process because they are specific (i.e., CA4/dentate gyrus and CA1 but not CA2/3 and the subiculum) and because the annualized rate of hippocampal atrophy measured ($-5.9\%/year$) is clearly above what can be observed on average in the healthy population ($-0.4\%/year$ in people <55 years old) (Fraser, Shaw, & Cherbuin, 2015). Another limitation is the short follow-up period (1-year), which was nonetheless long enough to capture the sequential progression of hippocampal subfield atrophy. We also acknowledge that we did not assess the potential microstructural damage that underlies or precedes hippocampal regional atrophy, with sequences such as diffusion-tensor imaging or magnetization transfer MRI, but these techniques are difficult to implement at the spatial resolution required to study hippocampal subfields. The final limitation was that, although no area of T2-hypersignal or T1-black hole was clearly detected within the hippocampus on our conventional sequences, we did not assess potential subtle demyelinating hippocampal lesions with specific double inversion recovery sequences.

5 | CONCLUSION

We demonstrated that CA4/dentate gyrus is the first subfield of the hippocampus to be atrophied during the course of MS, from the stage of CIS. This regional pattern of hippocampal atrophy rapidly spread to CA1. This dynamic vulnerability is associated with future diagnosis of MS and contributes to hippocampal-dependent memory performance.

STUDY FUNDING

This study was funded by the ARSEP Foundation, Bordeaux University Hospital, and TEVA Laboratories. The work was further supported by public grants from the French Agence Nationale de la Recherche within the context of the Investments for the Future program referenced ANR-10-LABX-57, named TRAIL (project IBIO-NI, GM-COG and HR-DTI), ANR-10-LABX-43, named BRAIN (Project MEMO-MS), ANR-10-IDEX-03-02, named IdEx Bordeaux - CPU, ANR-10-COHO-002, named French Observatoire for multiple sclerosis (OFSEP), and the CNRS multidisciplinary project "Défi ImagIn" HL-MRI. This research was also funded by Spanish UPV2016-0099 and TIN2013-43457-R grants from UPV and the Ministerio de Economía y competitividad. The sponsors did not participate in any aspect of the design or performance of the study, including data collection, management, analysis,

and the interpretation or preparation, review, and approval of the manuscript.

ACKNOWLEDGMENT

The authors thank Julie Charré-Morin and Aurore Saubusse (Bordeaux University Hospital) for neuropsychological testing and the ARSEP Foundation for its support.

DISCLOSURES

VP received a research grant from the ARSEP Foundation to conduct this study; he received travel expenses and/or consulting fees from Biogen, Teva-Lundbeck, and Merck-Serono unrelated to the submitted work. BB serves on scientific advisory boards on behalf of his institution and has received honoraria or research support from Biogen-Idec, Merck-Serono, Novartis, Genzyme, Teva, Roche, Medday, and Bayer unrelated to the submitted work. AR received research grants and/or consulting fees from Novartis, Biogen, Merck-Serono, Bayer Healthcare, Roche, Teva, and Genzyme unrelated to the submitted work.

ORCID

Vincent Planche  <http://orcid.org/0000-0003-3713-227X>

Pierrick Coupé  <http://orcid.org/0000-0003-2709-3350>

REFERENCES

- Avants, B. B., Tustison, N. J., Song, G., Cook, P. A., Klein, A., & Gee, J. C. (2011). A reproducible evaluation of ANTs similarity metric performance in brain image registration. *NeuroImage*, *54*, 2033–2044.
- Bakker, A., Kirwan, C. B., Miller, M., & Stark, C. E. L. (2008). Pattern separation in the human hippocampal CA3 and dentate gyrus. *Science*, *319*, 1640–1642.
- Coupé, P., Manjón, J. V., Chamberland, M., Descoteaux, M., & Hiba, B. (2013). Collaborative patch-based super-resolution for diffusion-weighted images. *NeuroImage*, *83*, 245–261.
- De Stefano, N., Airas, L., Grigoriadis, N., Mattle, H. P., O'riordan, J., Oreja-Guevara, C., ... Kieseier, B. C. (2014). Clinical relevance of brain volume measures in multiple sclerosis. *CNS Drugs*, *28*, 147–156.
- Du, A. T., Schuff, N., Kramer, J. H., Ganzer, S., Zhu, X. P., Jagust, W. J., ... Weiner, M. W. (2004). Higher atrophy rate of entorhinal cortex than hippocampus in AD. *Neurology*, *62*, 422–427.
- Dutta, R., Chang, A., Doud, M. K., Kidd, G. J., Ribaldo, M. V., Young, E. A., ... Trapp, B. D. (2011). Demyelination causes synaptic alterations in hippocampi from multiple sclerosis patients. *Annals of Neurology*, *69*, 445–454.
- de Flores, R., La Joie, R., & Chételat, G. (2015). Structural imaging of hippocampal subfields in healthy aging and Alzheimer's disease. *Neuroscience*, *309*, 29–50.
- Fraser, M. A., Shaw, M. E., & Cherbuin, N. (2015). A systematic review and meta-analysis of longitudinal hippocampal atrophy in healthy human ageing. *NeuroImage*, *112*, 364–374.
- Frisoni, G. B., Ganzola, R., Canu, E., Rüb, U., Pizzini, F. B., Alessandrini, F., ... Thompson, P. M. (2008). Mapping local hippocampal changes in Alzheimer's disease and normal ageing with MRI at 3 Tesla. *Brain: A Journal of Neurology*, *131*, 3266–3276.
- Gold, S. M., Kern, K. C., O'connor, M.-F., Montag, M. J., Kim, A., Yoo, Y. S., ... Sicotte, N. L. (2010). Smaller cornu ammonis 2–3/dentate

- gyrus volumes and elevated cortisol in multiple sclerosis patients with depressive symptoms. *Biological Psychiatry*, 68, 553–559.
- Habbas, S., Santello, M., Becker, D., Stubbe, H., Zappia, G., Liaudet, N., ... Volterra, A. (2015). Neuroinflammatory TNF α impairs memory via astrocyte signaling. *Cell*, 163, 1730–1741.
- Hulst, H. E., Schoonheim, M. M., Van Geest, Q., Uitdehaag, B. M. J., Barkhof, F., & Geurts, J. J. G. (2015). Memory impairment in multiple sclerosis: Relevance of hippocampal activation and hippocampal connectivity. *Multiple Sclerosis Journal*, 21, 1705–1712.
- Jack, C. R., Petersen, R. C., Xu, Y., O'Brien, P. C., Smith, G. E., Ivnik, R. J., ... Kokmen, E. (2000). Rates of hippocampal atrophy correlate with change in clinical status in aging and AD. *Neurology*, 55, 484–489.
- Jack, C. R., Barkhof, F., Bernstein, M. A., Cantillon, M., Cole, P. E., Decarli, C., ... Foster, N. L. (2011). Steps to standardization and validation of hippocampal volumetry as a biomarker in clinical trials and diagnostic criterion for Alzheimer's disease. *Alzheimers Dementia*, 7, 474–485.e4.
- Kerchner, G. A., Bernstein, J. D., Fenesy, M. C., Deutsch, G. K., Saranathan, M., Zeineh, M. M., & Rutt, B. K. (2013). Shared vulnerability of two synaptically-connected medial temporal lobe areas to age and cognitive decline: A seven tesla magnetic resonance imaging study. *The Journal of Neuroscience: The Official Journal of the Society for Neuroscience*, 33, 16666–16672.
- La Joie, R., Fouquet, M., Mézenge, F., Landeau, B., Villain, N., Mevel, K., ... Chételat, G. (2010). Differential effect of age on hippocampal subfields assessed using a new high-resolution 3T MR sequence. *NeuroImage*, 53, 506–514.
- Longoni, G., Rocca, M. A., Pagani, E., Riccitelli, G. C., Colombo, B., Rodegher, M., ... Filippi, M. (2015). Deficits in memory and visuospatial learning correlate with regional hippocampal atrophy in MS. *Brain Structure and Function*, 220, 435–444.
- Manjón, J. V., & Coupé, P. (2016). volBrain: An online MRI brain volumetry system. *Frontiers in Neuroinformatics*, 10, 30.
- Manjón, J. V., Coupé, P., Martí-Bonmatí, L., Collins, D. L., & Robles, M. (2010). Adaptive non-local means denoising of MR images with spatially varying noise levels. *Journal of Magnetic Resonance Imaging*, 31, 192–203.
- Manjón, J. V., Eskildsen, S. F., Coupé, P., Romero, J. E., Collins, D. L., & Robles, M. (2014). Nonlocal intracranial cavity extraction. *International Journal of Biomedical Imaging*, 2014, 820205.
- Maruszak, A., & Thuret, S. (2014). Why looking at the whole hippocampus is not enough—a critical role for anteroposterior axis, subfield and activation analyses to enhance predictive value of hippocampal changes for Alzheimer's disease diagnosis. *Frontiers in Cellular Neuroscience*, 8, 95.
- Miller, D. H., Chard, D. T., & Ciccarelli, O. (2012). Clinically isolated syndromes. *The Lancet. Neurology*, 11, 157–169.
- Morra, J. H., Tu, Z., Apostolova, L. G., Green, A. E., Avedissian, C., Madsen, S. K., ... Thompson, P. M. Alzheimer's Disease Neuroimaging Initiative (2009). Automated 3D mapping of hippocampal atrophy and its clinical correlates in 400 subjects with Alzheimer's disease, mild cognitive impairment, and elderly controls. *Human Brain Mapping*, 30, 2766–2788.
- Nyúl, L. G., & Udupa, J. K. (1999). On standardizing the MR image intensity scale. *Magnetic Resonance in Medicine*, 42, 1072–1081.
- Papadopoulos, D., Dukes, S., Patel, R., Nicholas, R., Vora, A., & Reynolds, R. (2009). Substantial archaocortical atrophy and neuronal loss in multiple sclerosis. *Brain Pathology*, 19, 238–253.
- Pérez-Miralles, F., Sastre-Garriga, J., Tintoré, M., Arrambide, G., Nos, C., Perkal, H., ... Montalban, X. (2013). Clinical impact of early brain atrophy in clinically isolated syndromes. *Multiple Sclerosis Journal*, 19, 1878–1886.
- Planche, V., Ruet, A., Coupé, P., Lamargue-Hamel, D., Deloire, M., Pereira, B., ... Tourdias, T. (2017a). Hippocampal microstructural damage correlates with memory impairment in clinically isolated syndrome suggestive of multiple sclerosis. *Multiple Sclerosis Journal*, 23, 1214–1224.
- Planche, V., Panatier, A., Hiba, B., Ducourneau, E.-G., Raffard, G., Dubourdieu, N., ... Tourdias, T. (2017b). Selective dentate gyrus disruption causes memory impairment at the early stage of experimental multiple sclerosis. *Brain, Behavior, and Immunity*, 60, 240–254.
- Planche, V., Ruet, A., Charré-Morin, J., Deloire, M., Brochet, B., & Tourdias, T. (2017c). Pattern separation performance is decreased in patients with early multiple sclerosis. *Brain and Behavior*, 7(8), e00739.
- Polman, C. H., Reingold, S. C., Banwell, B., Clanet, M., Cohen, J. A., Filippi, M., ... Wolinsky, J. S. (2011). Diagnostic criteria for multiple sclerosis: 2010 revisions to the McDonald criteria. *Annals of Neurology*, 69, 292–302.
- Rocca, M. A., Longoni, G., Pagani, E., Boffa, G., Colombo, B., Rodegher, M., ... Filippi, M. (2015). In vivo evidence of hippocampal dentate gyrus expansion in multiple sclerosis. *Human Brain Mapping*, 36, 4702–4713.
- Romero, J. E., Coupe, P., & Manjón, J. V. (2016). High resolution hippocampus subfield segmentation using multispectral multiatlas patch-based label fusion. In: *Patch-Based Techniques in Medical Imaging. Lecture Notes in Computer Science* (pp 117–124). Springer, Cham.
- Romero, J. E., Coupé, P., & Manjón, J. V. (2017). HIPS: A new hippocampus subfield segmentation method. *NeuroImage*, 163, 286–295.
- Schmidt, P., Gaser, C., Arsic, M., Buck, D., Förschler, A., Berthele, A., ... Mühlau, M. (2012). An automated tool for detection of FLAIR-hyperintense white-matter lesions in Multiple Sclerosis. *NeuroImage*, 59, 3774–3783.
- Sicotte, N. L., Kern, K. C., Giesser, B. S., Arshanapalli, A., Schultz, A., Montag, M., ... Bookheimer, S. Y. (2008). Regional hippocampal atrophy in multiple sclerosis. *Brain: A Journal of Neurology*, 131, 1134–1141.
- Small, S. A. (2014). Isolating pathogenic mechanisms embedded within the hippocampal circuit through regional vulnerability. *Neuron*, 84, 32–39.
- Stark, S. M., Yassa, M. A., Lacy, J. W., & Stark, C. E. L. (2013). A task to assess behavioral pattern separation (BPS) in humans: Data from healthy aging and mild cognitive impairment. *Neuropsychologia*, 51, 2442–2449.
- Thompson, P. M., Hayashi, K. M., De Zubicaray, G. I., Janke, A. L., Rose, S. E., Semple, J., ... Toga, A. W. (2004). Mapping hippocampal and ventricular change in Alzheimer disease. *NeuroImage*, 22, 1754–1766.
- Tustison, N. J., Avants, B. B., Cook, P. A., Zheng, Y., Egan, A., Yushkevich, P. A., & Gee, J. C. (2010). N4ITK: Improved N3 bias correction. *IEEE Transactions on Medical Imaging*, 29, 1310–1320.
- Wang, L., Swank, J. S., Glick, I. E., Gado, M. H., Miller, M. I., Morris, J. C., & Csernansky, J. G. (2003). Changes in hippocampal volume and shape across time distinguish dementia of the Alzheimer type from healthy aging. *NeuroImage*, 20, 667–682.
- West, M. J., Coleman, P. D., Flood, D. G., & Troncoso, J. C. (1994). Differences in the pattern of hippocampal neuronal loss in normal ageing and Alzheimer's disease. *Lancet (London, England)*, 344, 769–772.
- Winterburn, J. L., Pruessner, J. C., Chavez, S., Schira, M. M., Lobaugh, N. J., Voineskos, A. N., & Chakravarty, M. M. (2013). A novel in vivo

atlas of human hippocampal subfields using high-resolution 3 T magnetic resonance imaging. *NeuroImage*, 74, 254–265.

Wisse, L. E. M., Daugherty, A. M., Olsen, R. K., Berron, D., Carr, V. A., Stark, C. E. L., ... la Joie, R. Hippocampal Subfields Group (2017). A harmonized segmentation protocol for hippocampal and parahippocampal subregions: Why do we need one and what are the key goals? *Hippocampus*, 27, 3–11.

Yushkevich, P. A., Amaral, R. S. C., Augustinack, J. C., Bender, A. R., Bernstein, J. D., Boccardi, M., ... Zeineh, M. M. Hippocampal Subfields Group (HSG) (2015). Quantitative comparison of 21 protocols for labeling hippocampal subfields and parahippocampal subregions in in vivo MRI: Towards a harmonized segmentation protocol. *NeuroImage*, 111, 526–541.

SUPPORTING INFORMATION

Additional Supporting Information may be found online in the supporting information tab for this article.

How to cite this article: Planche V, Koubiyr I, Romero JE, et al. Regional hippocampal vulnerability in early multiple sclerosis: Dynamic pathological spreading from dentate gyrus to CA1. *Hum Brain Mapp.* 2018;39:1814–1824. <https://doi.org/10.1002/hbm.23970>